Atmospheric Pollution Research 13 (2022) 101544

Contents lists available at ScienceDirect

Atmospheric Pollution Research

journal homepage: www.elsevier.com/locate/apr

Study on the control of condensable particulate matter by spraying activated carbon combined with electrostatic precipitator

Zhenyao Xu, Yujia Wu, Xinlei Huang, Siqi Liu, Minghui Tang, Shengyong Lu *

State Key Laboratory of Clean Energy Utilization, Institute for Thermal Power Engineering, Zhejiang University, Hangzhou, 310027, China

ARTICLE INFO

Keywords:
Condensable particulate matter
Activated carbon
Adsorption

ABSTRACT

Condensable particulate matter (CPM) is a primary particulate matter that exists in the form of gas or vapor phase before discharge, but after discharge, it rapidly turns into a particulate substance due to cooling and dilution. The composition of CPM is very complex, and it poses a threat to the environment and human health. However, there is a lack of research on the control of CPM. Therefore, this study investigated the effects of activated carbon (AC) injection coupled with low-low temperature electrostatic precipitator on the adsorption of CPM in the flue gas of a 300 MW ultra-low emission coal-fired power plant. The sampling system was conducted according to ISO 23210–2009 and U.S. EPA method 202. Results shows that the adsorption removal efficiency of CPM by ACs ranged from 14% to 33%, and the adsorption removal effect of AC on inorganic components in CPM was better than that of organic components. AC had significant adsorption effects on Cl^- and NH_4^+ but had weak adsorption effect on NO_3^- in CPM. AC with larger specific surface area, more abundant pore structure, and richer surface chemical functional groups has better adsorption effect on metal elements such as Na, Ca, Mg, K, and Al in CPM is better than that of Fe. As for the organic components in CPM, the adsorption effect of AC for esters was considerable, but its adsorption on organosilicon was limited.

1. Introduction

Condensable particulate matter (CPM) is a primary particle that exists in the form of gas or vapor phase at flue gas temperature before discharge but turns into a particulate substance after dilution and cooling in the plume (Li et al., 2021; Wang et al., 2018; Wu et al., 2021a). Significantly, CPM is also a kind of PM with aerodynamic diameter less than 2.5 μm, which belongs to the category of $PM_{2.5}$ (Wang et al., 2020a; Yang et al., 2018). Because of its large specific surface area, CPM can absorb toxic substances and harmful pollutants. When it enters the human body through the respiratory system, it will not only harm the respiratory system but also lead to asthma, bronchitis, and cardiovascular diseases (Feng et al., 2018; Liu et al., 2022). In addition, CPM will reduce the visibility of the atmosphere, resulting in an increase in haze weather (Morino et al., 2018; Wang et al., 2018).

In recent years, the pollutant emission standards of coal-fired power plants have been gradually tightened, especially in China, which has issued ultra-low emission standards (PM < 5 mg/Nm^3; CPM is not included) (Li et al., 2016, 2017). Predecessors have also done some research on the removal effect of CPM by air pollution control devices (APCDs). Qi et al. (2017) and Li et al. (2019) concluded that low-low temperature electrostatic precipitator (LLT-ESP) had a remarkable removal efficiency for CPM, with CPM removal efficiencies of more than 60%. Wang et al. (2020b) investigated the effect of wet flue gas desulfurization (WFGD) system and wet electrostatic precipitator (WESP) system on CPM in four typical coal-fired power plants, and they found WFGD system was more effective in reducing CPM than WESP. Liu et al. (2022) summarized the removal effect of WFGD on CPM in four coal-fired power plants, with the removal efficiency range is 27%–39%. However, the concentration of CPM discharged from the flue gas emission of coal-fired power plants is still range from 43.74 mg/Nm^3 to 90.6 mg/Nm^3 (Wu et al., 2021a), indicating that the removal effect of traditional APCDs on CPM is limited, resulting in the emission of CPM far exceeding the ultra-low emission standard (Cano et al., 2017; Li et al., 2017; Song et al., 2020; Yang et al., 2019; Zheng et al., 2018). However, there is a lack of techniques for controlling CPM, so it is urgent to seek the technology to control CPM.

Two possible development directions for controlling CPM from coal

Peer review under responsibility of Turkish National Committee for Air Pollution Research and Control.
* Corresponding author.
E-mail address: lushy@zju.edu.cn (S. Lu).

https://doi.org/10.1016/j.apr.2022.101544
Received 23 June 2022; Received in revised form 20 August 2022; Accepted 25 August 2022
Available online 1 September 2022
1309-1042/© 2022 Turkish National Committee for Air Pollution Research and Control. Production and hosting by Elsevier B.V. All rights reserved.

burning are removal by cooling condensation and adsorbent adsorption (Feng et al., 2018). As an important air pollution treatment method, adsorption has already been used widely because it is simple and efficient. Carbon materials are considered to be the most potential adsorbent with low cost, high efficiency and good stability, although they have inherent defects such as hygroscopicity and pore blockage (Bradley, 2011). Activated carbon (AC) is produced from carbon-rich materials by the processes of carbonization and activation (Zhang et al., 2017). And it is one of the most popular adsorbents because of its low cost, strong adsorption capacity, acid, and alkali resistance and heat resistance. There are a large number of studies on the application of AC in combined desulfurization, denitrification, and mercury removal of power plant flue gas (Chen et al., 2019, 2021; Tang et al., 2005; Chi, 2018). AC is also widely used to study the adsorption of volatile organic pollutants because of its various advantages (Chiang et al., 2001; Giraudet et al., 2014; Qian et al., 2015). And some scholars have studied the adsorption of polycyclic aromatic hydrocarbons by AC and found that AC has a good adsorption effect on it (Zhou et al., 2005). In addition, the research on the removal of dioxins in the flue gas of waste incineration plant by AC combined with bag filter shows that AC has an excellent removal effect on dioxins in the flue gas, and the AC with richer mesopores, larger micropores, and average mesopores has better adsorption effect on 2,3,7,8-PCDD/Fs (Qing et al., 2017). Besides, previous studies have found that the composition of CPM is very complex, in which the inorganic components contain water-soluble ions such as SO_4^{2-}, Cl^-, and metal elements such as Na, K, Ca, and Al, as well as rich organic components, including alkanes, esters and so on (Feng et al., 2018). And AC is an excellent adsorbent and can adsorb a variety of substances, while CPM is a complex material containing many components. Therefore, AC is used as an adsorbent to adsorb CPM to carry out the research in this paper.

Combined with the existing flue gas pollutant treatment process of coal-fired power plants, AC injection coupled with an electrostatic precipitator (ESP) is a relatively simple and feasible method for the removal of CPM. This method does not need to purchase additional large-scale equipment, but only needs to add injection points in front of the existing ESP, which greatly reduces the operation cost. In this work, CPM samples were collected from a domestic ultra-low emission coal-fired power plant to study the effects of the type and amount of ACs coupled with ESP on the adsorption of CPM in the flue gas. The distribution characteristics of CPM at the inlet and outlet of ESP were discussed, and the adsorption of water-soluble ions and metal elements in CPM by AC was analyzed. In addition, the changes in organic components in CPM before and after AC injection were also compared and studied. The work of this paper provides some guidance and direction for the AC adsorption and control of CPM.

2. Materials and methods

2.1. Facility, sampling sites, and methods

This study was conducted in a 300 MW ultra-low emission coal-fired power plant, which was equipped with a selective catalytic reduction (SCR) denitration device, an LLT-ESP, a WFGD system, and a WESP. The LLT-ESP combines with three rooms and four electric fields, and a non-leakage media gas-gas exchanger (MGGH) (Li et al., 2019), which reduces the flue gas temperature at the inlet of the ESP from the conventional 120–160 to the low-low temperature state (generally about 85–95) below the acid dew point (Shou et al., 2016). The sampling sites were located before and after ESP, as shown in Fig. 1, which shows a schematic diagram of LLT-ESP as well. The particulate matter samples under three test conditions were collected. First, the samples before and after the ESP without spraying adsorbent. Second, the samples at two sampling sites when 50 mg/m^3 and 150 mg/m^3 wood AC were sprayed before the ESP (named ACM-50 and ACM-150), and finally, the samples when 150 mg/m^3 coconut shell AC was sprayed were collected as well

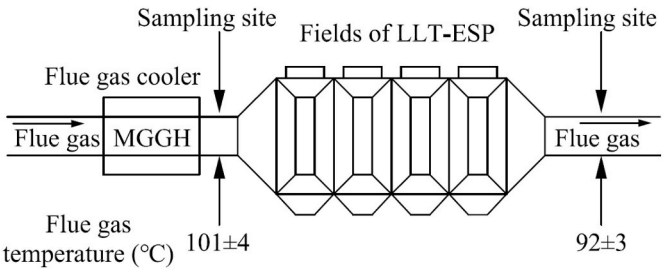

Fig. 1. Schematic diagram and sampling sites of LLT-ESP.

(named ACY-150). And the load of the coal-fired unit was maintained at 300 MW during the sampling period. In addition, in order to ensure the reliability of data, each sampling site was sampled twice at least. And the results of proximate and ultimate analyses of pulverized coal used by coal-fired units during sampling are shown in Table 1.

The schematic diagram of the system for collecting CPM from flue gas is shown in Fig. S1. The system was comprised of an FPM collection system and a CPM collection system, which can sample FPM and CPM from flue gas at the same time. Before the flue gas entered the CPM collection system, the temperature of the flue gas would be maintained at about 130 °C by the temperature control box and heating belt. This could guarantee that the CPM samples were not affected by moisture. In order to ensure the smooth progress of on-site sampling, the flow of the induced draft fan was set to 10 L/min. For a more detailed description of the functions and sampling process of the system, refer to the previous studies of our team (Wu et al., 2021a, b; Xu et al., 2022).

2.2. Analytical procedure for samples

The collection and analysis of CPM samples were based on U.S. EPA Method 202 (United Stated, 2016). Organic and inorganic samples can be obtained through on-site collection and laboratory pretreatment analysis. The specific operation process and pretreatment methods have been described in detail in previous studies (Wu et al., 2021a, b). The sum of organic and inorganic components was the mass of CPM, and then the mass concentration of CPM in flue gas could be calculated according to the volume of flue gas collected. After that, the organic and inorganic extracts of CPM samples were ultrasonically dissolved with n-hexane and deionized water to 10 ml and then stored for later use.

After the concentration of the total PM mass analysis, chemical analysis for organic and inorganic components of CPM samples were carried out. The organic extracts in CPM were detected by gas chromatography/mass spectrometry (GC/MS) for qualitative and semi-quantitative analysis. The specific instrument model, parameter setting and temperature rise program can refer to the previous research results of our laboratory (Li et al., 2017; Song et al., 2020; Wu et al., 2021c). For the detection of inorganic ions of CPM, the concentration of anions such as SO_4^{2-}, NO_3^-, Cl^- and F^- was quantitatively measured by ion chromatograph (IC: DIONEX AQUION), and the concentration of NH_4^+ ions was also measured by it. The metal cations such as Na, Ca, Mg, K, Fe, and Al in the CPM were detected by inductively coupled plasma mass spectrometry (ICP-MS: PerkinElmer NexION 300*X*). When detecting each ion, it is necessary to detect the standard sample at the same time, so as to draw the calibration curve. The R^2 of the calibration curves needs to be greater than 0.99 to ensure accuracy. It is worth noting that when inorganic samples enter the testing instruments, there must be no organic components present. Therefore, the inorganic solution should be filtered with a specific filter membrane before detection to remove the possible organic matter. In addition, in order to avoid excessive contamination of the detection instrument by the ions to be measured in the solution, the inorganic solution needs to be diluted to the corresponding multiple.

Table 1
Details of the Coal parameters.

	Proximate Analyses (%)				Ultimate Analyses (%)					Q_{net}
Sample	M_{ad}	A_{ad}	V_{ad}	FC_{ad}	C_{ad}	H_{ad}	N_{ad}	$S_{t,ad}$	O_{ad}	(MJ/kg)
Bituminous Coal	3.04	32.29	15.14	49.53	56.53	2.60	0.75	2.48	2.31	21.08

[a]Note: ad = air dry basis, M = moisture content, A = ash content, V = volatile content, FC = fixed carbon, S_t = total sulfur, and Q_{net} = net calorific value.

2.3. Characterization of ACs

2.3.1. Surface area and pore width distribution

The pore size of AC can be divided into three categories according to the International Union of Pure and Applied Chemistry (IUPAC), micropore (pore size <2 nm), mesopore (2–50 nm), and macropore (>50 nm). Micropores contribute to the surface area, while macropores can act as channels to contribute to the micropore surface (Yahya et al., 2015). The AC used in the field test are wood based AC (abbreviated as ACM) and coconut shell based AC (abbreviated as ACY) respectively. The pore characterizations of two kinds of ACs are presented in Table 2, in order to more intuitively show the difference between the two ACs, the pore size distributions of micropores and mesopores (0.6–50 nm) derived from N_2 adsorption/desorption isotherms are shown in Fig. 2. It can be seen from Table 2 that ACY has a larger BET surface area of 1282 m^2/g than ACM, and the pore volume of ACY is more than twice that of ACM. This phenomenon can also be clearly observed in Fig. 2. Fig. 2(a) displayed the pore size distribution curves of ACs calculated by the BJH model, from which it can be found that ACY exhibited higher mesopore content. From Table 2, it can also be seen that the mesoporous volume of ACY is more than five times that of ACM. Besides, the pore size distribution curves calculated according to the DFT model are shown in Fig. 2 (b). Combined with the data of pore volume in Table 2, it can be found that there is little difference in micropore volume between the two ACs. Combined with the results of Fig. 2(a) and (b), it can be concluded that ACY has abundant micropores and mesopores ranging from 1 to 50 nm.

2.3.2. Functional groups of ACs

To investigate the chemical compositions and the surface functional groups of ACs, the X-ray photoelectron spectroscopy (XPS) analysis of two ACs was carried out and the results are shown in Table S1 and Fig. S2. Table S1 shows that the C-Atoms% of the ACM is 93.35%, which is higher than that of ACY. As presented in Fig. S2(a), the wide scan spectrum shows three main peaks at about 285 and 532 eV, which are assigned to C1s and O1s spin-orbit couplings respectively. The spectra of C1s can be deconvoluted into three subpeaks, including C–C (284.2–284.9 eV), C–O (285.4–285.9 eV), and C═O (286.2–287.9 eV) (Wang et al., 2020c). Table S1 exhibits the ratios of three different surface functional groups of two AC samples in this field test. The proportion of the C–O bond in AC with higher oxygen element is higher, and the content of carbon element in ACM is higher, so the proportion of the C–C bond on its surface is higher, and the proportion of C═C bond on the surface of the two ACs is almost the same. The increase of oxygen-containing functional groups on the surface of AC will improve the adsorption capacity and selectivity of metal ions, and also have a certain impact on the adsorption of organic substances (Meng et al., 2007). Ge et al. (2016) found that the less oxygen-containing groups, the better the removal effect of polycyclic aromatic hydrocarbons. And Chiang et al. (2002) found that the increase of oxygen-containing functional groups would greatly improve the adsorption capacity of AC for methylethylketone and benzene. Thus, it can be seen that different chemical functional groups have obvious adsorption differences for different adsorbates.

3. Results and discussion

3.1. Adsorption effects on CPM of ACs

The concentrations of CPM samples were the average values calculated from continuous samples. And the data results have been converted to standard concentrations at 6% oxygen, dry standard conditions, according to GB/T 16157–1996 and GB 13223-2011 before further analysis.

The mass concentrations of CPM and its organic and inorganic components before and after adsorption were listed in Table 3. In order to more intuitively show the influence of ACs, the concentrations of CPM were drawn into a histogram as shown in Fig. 3. When ACs were not sprayed before LLT-ESP, the concentrations of CPM in flue gas at the inlet and outlet of LLT-ESP were 143.09 mg/Nm^3 and 47.92 mg/Nm^3 respectively. And Fig. 3 illustrated that the LLT-ESP had a certain effect on removing the organic and inorganic components of CPM, but it could not meet the requirements of ultra-low emission. Formula 1 was used to calculate the adsorption efficiency of different ACs to different components, in which $\eta_{ACs\cdot component}$ is the adsorption efficiency of different ACs for different components, $C_{ACs\cdot component}$ and $C_{outlet\cdot component}$ are the concentrations of the component at the outlet of LLT-ESP when AC is sprayed and not sprayed, respectively. Two kinds of ACs were used to adsorb CPM at two different injection rates, comparing the difference of CPM emission concentration when the same AC was sprayed, the results showed that appropriately increasing the injection amount of adsorbent could reduce the emission concentration of CPM at the outlet of LLT-ESP. And the adsorption efficiency of CPM and of its organic and inorganic fractions was showed in Fig. 4, the adsorption removal efficiency of CPM ranged from 14% to 33%. It can be observed from Fig. 4 that when 150 mg/m^3 coconut shell AC was sprayed, the adsorption removal efficiency of CPM was 32.08%, which had the best adsorption effect on CPM under the three spraying conditions. Combined with the characterization data of ACs in Table 2, it is found that the AC with a larger specific surface area and richer pore volume has a better adsorption effect on CPM. However, this does not mean that the kinds and amount of chemical functional groups in ACs have little impact on the adsorption of CPM. After all, the components in CPM were diverse and complex, and the specific impact would be analyzed for different components in the following sections. As indicated in Fig. 4, the adsorption removal efficiency ranges of organic and inorganic components of CPM were 9%–27% and 32%–52%, respectively. Such results suggested that the adsorption removal effect of ACs on inorganic components in CPM was better than that of organic components. That is because the temperature of LLT-ESP was between 105 °C and 135 °C, which was not very suitable for ACs to adsorb organic components (Zhang et al., 2017).

Table 2
Specific surface area and pore width distribution of two ACs.

Material	S_{BET} (m^2/g)	Micropore Area (m^2/g)	Pore volume (cm^3/g)	Micropore volume (cm^3/g)	Mesopore volume (cm^3/g)	Average pore size (nm)
ACM	922	544	0.479	0.223	0.091	2.08
ACY	1282	697	1.018	0.294	0.460	3.18

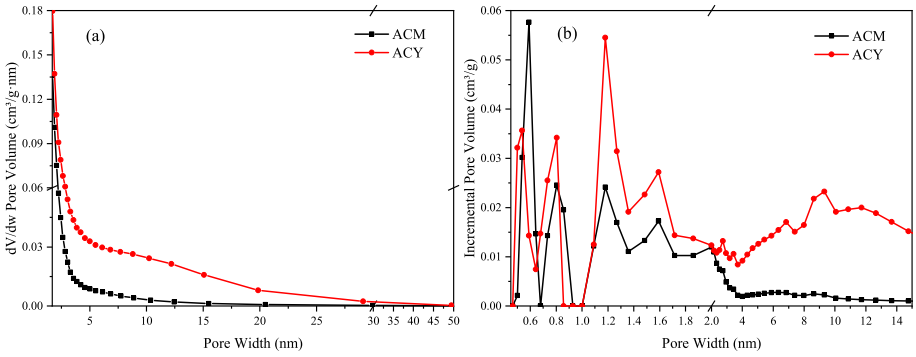

Fig. 2. Pore size distribution of ACM and ACY calculated by the (a) BJH model, (b) DFT model.

Table 3
The average concentrations of CPM before and after adsorption (mg/Nm^3).

Particulate matters	Inlet	Outlet	ACM-50	ACM-150	ACY-150
Organic fraction	92.76	37.99	35.29	33.02	28.47
Inorganic fraction	50.33	9.94	7.01	6.05	4.59
CPM	143.09	47.92	42.30	39.07	33.07

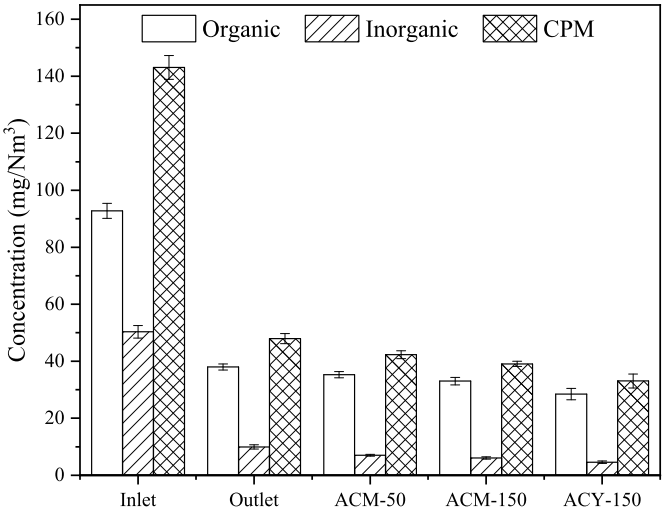

Fig. 3. The average concentrations of CPM before and after adsorption.

$$\eta_{ACs\text{-}component} = \frac{C_{outlet\text{-}component} - C_{ACs\text{-}component}}{C_{outlet\text{-}component}} \times 100\% \quad (1)$$

3.2. Water-soluble ion analysis

Existing studies have shown that water-soluble ions have an extinction effect on solar radiation, which aggravates the formation of haze (Wu et al., 2017). Moreover, water-soluble ions can easily enter the soil and water with rainfall and then pose a threat to the environment (Wang et al., 2021). Therefore, it is of great significance to study the changes of water-soluble ions in CPM before and after AC adsorption for controlling CPM and haze weather.

In this study, a series of water-soluble ions such as Cl^-, NH_4^+, SO_4^{2-}, F^-, NO_3^-, NO_2^- and PO_4^{3-} were detected, but the detection results showed that the concentrations of NO_2^- and PO_4^{3-} were significantly lower than other ions, so they were not discussed in the following sections. And the average concentrations of water-soluble ions in CPM at different sampling sites were shown in Table S2, which illustrated that the average emission concentrations of Cl^-, NH_4^+, SO_4^{2-}, F^-, and NO_3^- in CPM at the outlet of LLT-ESP were 447.58, 3365.82, 1475.45, 664.01, and 41.82

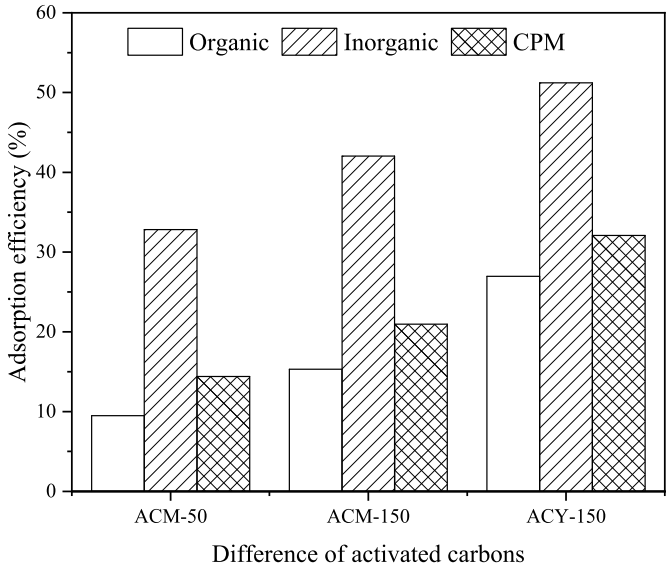

Fig. 4. Adsorption efficiency of different components by ACs.

μg/Nm^3, respectively. And the efficiency of these water-soluble ions adsorbed and removed by ACs in the field test was plotted in Fig. 5. It can be found from Fig. 5 that the ACs had a considerable adsorption

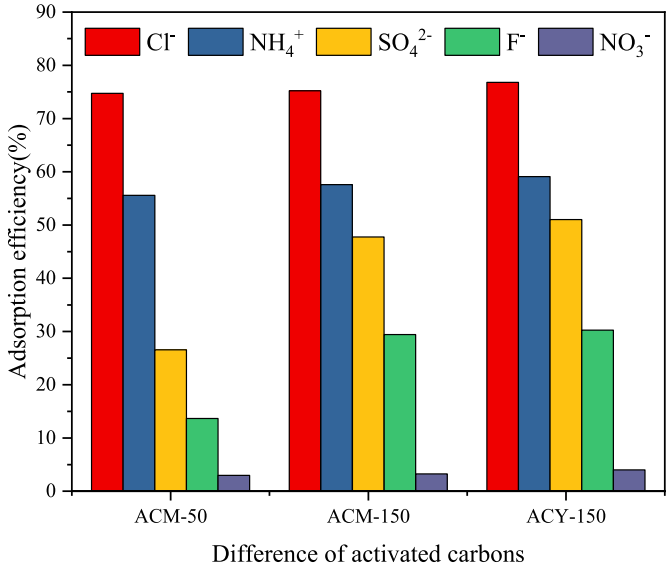

Fig. 5. Adsorption efficiency of water-soluble ions in CPM by ACs.

effect on Cl^- and NH_4^+, and the adsorption efficiency of them was maintained at about 75% and 57% respectively regardless of the kind of ACs or amount of ACs sprayed. In contrast, the adsorption efficiency of ACs on SO_4^{2-} was obviously related to the type of AC and the injection amount of AC. In addition, the adsorption efficiency of F^- was only related to the amount of AC injection. And it should be noted that the adsorption effect of ACs on NO_3^- was not satisfactory, and the adsorption efficiency was not more than 5% under three different conditions.

Ammonia will be produced in the process of coal combustion, and ammonia will also be introduced in the process of denitration. As a typical weak polar gas, ammonia is easily absorbed by AC, which is a natively nonpolar adsorbent (Zhang et al., 2017). Previous experiments on ammonia adsorption by AC have been carried out (Miyoshi et al., 1976), and it is found that the adsorption of ammonia by ACs mainly depends on the surface properties (pH and amount of base) of ACs, rather than their porous structure. Thus, when the flue gas flowed through AC, ammonia can react with hydroxyl, phenolic, and other acidic functional groups on AC, so the concentration of NH_4^+ in the collected CPM is reduced. In addition, researchers modified AC with HNO_3 to increase the content of acidic groups on its surface and the results showed that the adsorption capacity of ammonia was increased by 36.98% (Sheng et al., 2010).

The Cl^- in CPM mainly comes from HCl in flue gas, which is produced by the combustion and gasification of high volatile chlorine in coal (Sun et al., 2021). The previous study shows that AC has an excellent adsorption effect on HCl, and its adsorption effect is related to the oxygen-containing functional groups on the carbon surfaces (Park and Kim, 2004). The distribution of functional groups on the surface of the two ACs used in this study is similar, and the Cl^- content in CPM from the original flue gas is not very high, so the adsorption efficiency of Cl^- under the three conditions is basically the same. F^- and Cl^- belong to the same halogen group. Therefore, it is considered that there is little difference in the adsorption of F^- between the two ACs with similar surface functional groups. However, due to the higher concentration of F^- in the flue gas than Cl^-, the AC failed to fully adsorb F^- when the injection amount of AC was less, resulting in lower adsorption efficiency.

Sulfur and nitrogen in the flue gas of coal-fired power plant mainly exist in the form of SO_2 and NO_X. LLT-ESP is arranged behind the denitration equipment and before the desulfurization equipment in the coal-fired power plant. Therefore, the concentration of NOx in the flue gas here is lower and the concentration of SO_2 is relatively high. It was considered that only a few of the adsorption of SO_2 by AC existed on the inner surface of AC in the form of physical adsorption (Zhang, 2008). Therefore, there is no significant difference in SO_2 adsorption between the two ACs with similar a chemical bond distribution. Experimental research on AC synergistic desulfurization and denitrification was carried out (Zhu, 2015). The result showed that the higher concentration of SO_2 in the denitrification process, the worse the adsorption effect of AC on NO. Combined with the concentration difference of SO_2 and NO_X in CPM from flue gas mentioned before, it can explain the poor adsorption effect of ACs on NO_X under the three conditions. This research result can provide guidance for simultaneous desulfurization and denitrification of AC.

3.3. Metal elements analysis

Toxicological research shows that metal components will enter the human body through the circulatory system and respiratory system, which will not be degraded and cause a large amount of accumulation, which has toxic effects on the nervous system, immune system and reproductive system of the body (Chen and Lippmann, 2009; Sabeti et al., 2021). Therefore, measuring the adsorption of AC on metal elements in CPM is of great significance to control the pollution produced by fuel combustion.

In this work, six metal elements of Na, Mg, Al, K, Ca, and Fe were quantitatively detected, the results were listed in Table S3. When ACs were not sprayed, the concentrations of these six metal elements in CPM at the outlet of LLT-ESP were 219.29, 23.24, 75.16, 44.89, 205.15, and 27.26 μg/Nm^3, respectively. In order to more intuitively show the removal effect of ACs on each metal ion, the adsorption efficiency of AC on metal ions was plotted in Fig. 6, which shows that the adsorption effect of ACs on different metal ions was different. By observing Fig. 6, it can be found that coconut shell AC had a better adsorption effect on other metal elements except Fe. This is because the adsorption between the Ca, Na, K and the active site is physical adsorption (Ge et al., 2019), while Mg and Ca are congeneric metal elements, so it is speculated that the adsorption between Mg and the active site is also physical adsorption. Therefore, the AC with a larger specific surface area (ACY) has a better adsorption effect. In addition, the kinetic diameter of these metal elements is between 0.1 and 0.266 nm. According to Table 2, the microporous structure of ACY is more abundant, so its adsorption effect on the metal elements is better. From previous studies, it can be known that the adsorption of aluminum by AC is physical adsorption (Delgadillo-Velasco et al., 2021), and the kinetic diameter and ion radius of aluminum ions are the smallest among these metal elements. Therefore, ACY with more abundant microporous structure has significant adsorption effect on Al. Another obvious phenomenon from the figure is that ACY had a good adsorption effect on Na, Mg, and Al, with an adsorption efficiency of more than 40%. This is closely related to the small ion radius of Na, Mg and Al. And this result is similar to the previous research results (Zhang et al., 2021). Previous studies on the removal of Fe^{2+} by AC found that the texture parameters of AC are not the key factor affecting the adsorption of metals in water, but the surface chemistry may be the key factor affecting the adsorption (Queiroz et al., 2020). Although this study was carried out in an aqueous solution, water molecules also exist in the flue gas, so it can also be used to explain the phenomenon that the adsorption effects of the two ACs on Fe were similar in this work. The adsorption effect of AC on metal elements in flue gas is complex and unknown. This study only provides an idea and direction, and more and more in-depth research is needed.

3.4. Organic fraction analysis

Many studies in recent years have shown that organic components account for a large proportion in CPM from flue gas of coal-fired power plants (Feng et al., 2018; Li et al., 2017; Song et al., 2020; Wu et al., 2021a). The number of organic compounds in CPM is very large, and the composition is not clear, so it is difficult to quantitatively analyze the organic components in CPM. Therefore, the organic components in CPM

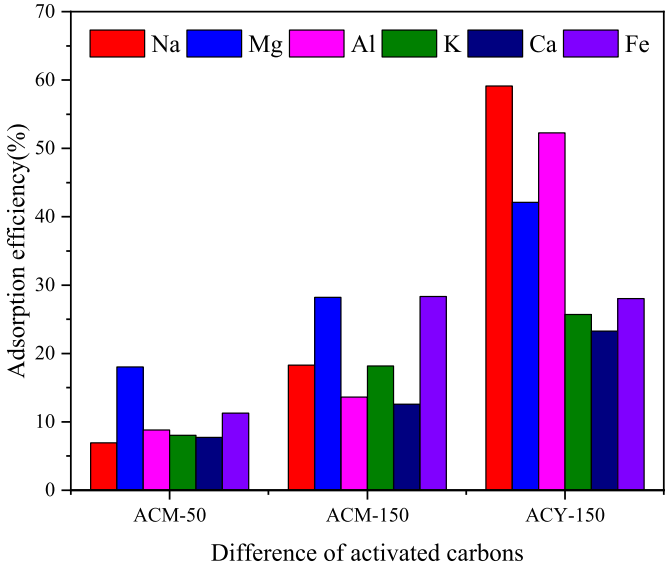

Fig. 6. Adsorption efficiency of metal elements in CPM by ACs.

were semi-quantitatively analyzed by gas chromatography-mass spectrometry (GC-MS) in this work. The test reports not only listed the name of hundreds of detected organic substances, but also included the retention time, CAS Number, molecular formula, and area proportion of each substance. In order to reveal the adsorption law of ACs on organic components of CPM, the peak areas of the same type of organic substances were combined to obtain data and plotted the proportion results as shown in Fig. 7.

As shown in Fig. 7, the organic substances in CPM could be roughly divided into the following five categories: esters, hydrocarbons, organosilicon, heteroatom containing compounds (contained heteroatoms except C, H, O, Si) and other organics. Other organics mainly included aldehydes, ketones, ethers, alcohols and other complex macromolecular organic compounds. It can be seen from Fig. 7 that the injection of ACs before LLT-ESP led to the change in the proportion of organic components in CPM, but it was difficult to quantify the change in different components. This difficulty needs to be overcome in the future, so as to analyze the specific impact of AC on different organic components in CPM. In addition, when the flue gas was adsorbed by ACs, the proportion of organosilicon in CPM was increased from 43.88% to 45.14%–55.92%, while the proportion of esters decreased by 2.85%–9.01%. Compare the effects of different types of activated carbon with the same injection amount on the proportion of organic substances in CPM, as shown in Fig. 7 (b) (d) (e), it can be found that the proportion of hydrocarbons in CPM increased to 30.92% by spraying wood AC, while the proportion decreased by 4.47% by spraying coconut shell AC. However, under these two conditions, the proportion of heteroatom containing organic compounds is completely opposite. According to the above phenomenon, it can be concluded that AC had a considerable effect on the removal of esters in CPM, thus reducing the proportion of esters in CPM. However, the removal effect of AC on organosilicon was limited. The adsorption effect of carbonaceous adsorbents is related to the molecular structure of the adsorbed organic matter, and those with small molecular sizes are easier to be adsorbed (Lashaki et al., 2012; Qian et al., 2015). Furthermore, the boiling point of organic matter is one of the key factors to influence the adsorption effect of ACs (Chiang et al., 2001; Giraudet et al., 2014). In this work, it is semi quantitatively detected that the molecular weight of organosilicon substances in CPM is significantly higher than that of esters, but the boiling point of esters is significantly higher than that of organosilicon substances. It is consistent with the previous research results. Some predecessors studied the adsorption effects of five different ACs on organic components in CPM in the laboratory (Zhang et al., 2021). The results showed that the proportion of alkanes, esters, and other organics in CPM in flue gas changed after adsorption of different ACs, and it was also found that all ACs had good adsorption effects on aromatic compounds in CPM. The study on the adsorption of aromatic compounds in CPM by ACs can pay close attention to the upcoming research results of our team. Using ACs to absorb organic matter is one of the important means to control organic pollutants. Therefore, predecessors have done a lot of research on the adsorption of organic pollutants by ACs, including alkane, esters, aromatics, alcohols, aldehydes, ethers, etc. The adsorption effect of AC on the organic matter is related to the physicochemical properties of AC, such as specific surface area, pore volume, pore distribution and chemical functional groups on its surface (Chiang et al., 2001; Zhang et al., 2017). These conclusions are helpful to understand the research results of this paper.

4. Conclusions

This study investigated the effects of the type and amount of ACs coupled with LLT-ESP on the adsorption of CPM in the flue gas of a 300 MW ultra-low emission coal-fired power plant. In this work, not only the distribution characteristics of CPM at the inlet and outlet of LLT-ESP were discussed, but also the composition of CPM before and after spraying ACs was analyzed. The adsorption removal efficiency of CPM by ACs reached 32.08%, reducing the mass concentration of CPM at the outlet of LLT-ESP from 47.92 mg/Nm^3 to 33.07 mg/Nm^3. In particular, ACs had a better adsorption removal effect on the inorganic components in CPM, with the adsorption removal efficiency range from 32% to 52%. ACs had considerable adsorption effects on Cl^- and NH_4^+ in the water-soluble ions of CPM but had a weak adsorption effect on NO_3^-, and the adsorption efficiency of them was maintained at about 75%, 57%, and 3% respectively regardless of the kind of ACs or amount of ACs sprayed. The coconut shell AC had a good adsorption effect on metal elements (Na, Ca, Mg, K, and Al) in CPM except Fe. Because ACY had a larger

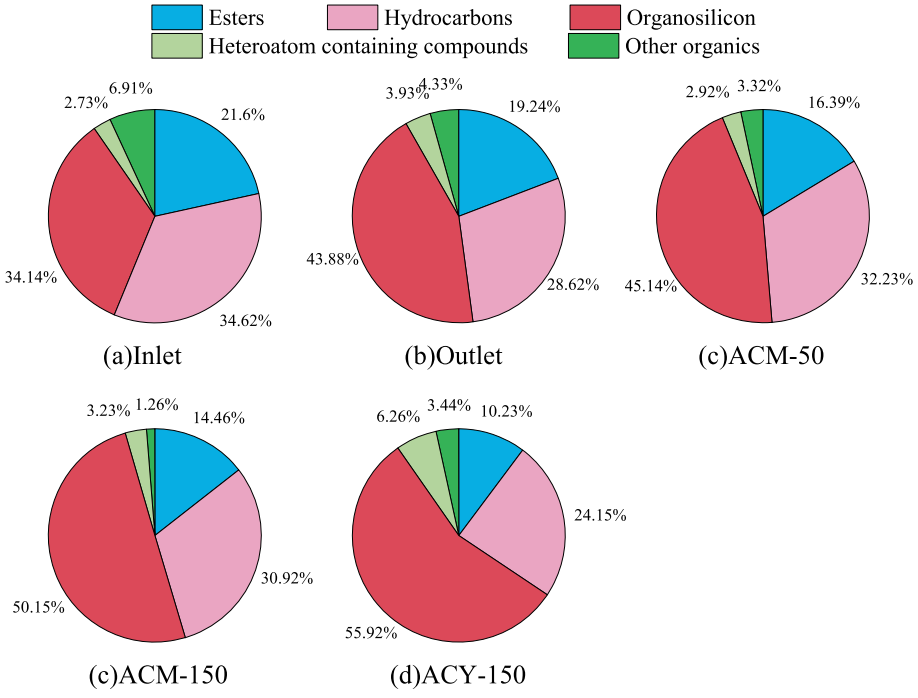

Fig. 7. Change in the ingredients in organic fractions before and after adsorption.

specific surface area, richer pore structure and chemical functional groups on its surface, it could facilitate the adsorption of these metal elements. The injection of ACs in LLT-ESP led to the change in the proportion of organic components in CPM. Besides, AC had a considerable effect on the removal of esters in CPM, but the removal of organosilicon was limited. This is because the molecular size of esters in CPM is smaller than that of organosilicon, but with a higher boiling point.

Credit author statement

Zhenyao Xu: Conceptualization, Formal analysis, Data curation, Writing – original draft. **Yujia Wu**: Methodology, Data curation. **Xinlei Huang**: Methodology, Data curation. **Siqi Liu**: Investigation. **Minghui Tang**: Methodology. **Shengyong Lu**: Supervision.

Declaration of competing interest

The authors declare that they have no known competing financial interests or personal relationships that could have appeared to influence the work reported in this paper.

Acknowledgement

The research was supported by the National Key Research and Development Program of China (2018YFB0605200).

Appendix A. Supplementary data

Supplementary data to this article can be found online at https://doi.org/10.1016/j.apr.2022.101544.

References

Bradley, R.H., 2011. Review recent developments in the physical adsorption of toxic organic vapours by activated carbons. Adsorpt. Sci. Technol.
Cano, M., Vega, F., Navarrete, B., Plumed, A., Camino, J.A., 2017. Characterization of emissions of condensable particulate matter in clinker kilns using a dilution sampling system. Energy Fuel. 31 (8), 7831–7838.
Chen, L.C., Lippmann, M., 2009. Effects of metals within ambient air particulate matter (PM) on human health. Inhal. Toxicol. 21 (1), 1–31.
Chen, C., Duan, Y., Zhao, S., Hu, B., Li, N., Yao, T., Zhao, Y., Wei, H., Ren, S., 2019. Experimental study on mercury removal and regeneration of SO_2 modified activated carbon. Ind. Eng. Chem. Res. 58 (29), 13190–13197.
Chen, R., Zhang, T., Guo, Y., Wang, J., Wei, J., Yu, Q., 2021. Recent advances in simultaneous removal of SO_2 and NO_X from exhaust gases: removal process, mechanism and kinetics. Chem. Eng. J. 420, 127588.
Chi, M., 2018. Experimental Study on Desulfurization, Denitrification and Mercury Removal by Activated Carbon. North China Electric Power University, p. 49.
Chiang, Y., Chiang, P., Huang, C., 2001. Effects of pore structure and temperature on VOC adsorption on activated carbon. Carbon 39 (4), 523–534.
Chiang, H.L., Chiang, P.C., Huang, C.P., 2002. Ozonation of activated carbon and its effects on the adsorption of VOCs exemplified by methylethylketone and benzene. Chemosphere 47 (3), 267–275.
Delgadillo-Velasco, L., Hernández-Montoya, V., Ramírez-Montoya, L.A., Montes-Morán, M.A., Del Rosario Moreno-Virgen, M., Rangel-Vázquez, N.A., 2021. Removal of phosphate and aluminum from water in single and binary systems using iron-modified carbons. J. Mol. Liq. 323, 114586.
Feng, Y., Li, Y., Cui, L., 2018. Critical review of condensable particulate matter. Fuel 224, 801–813.
Ge, X., Wu, Z., Wu, Z., Yan, Y., Cravotto, G., Ye, B., 2016. Enhanced PAHs adsorption using iron-modified coal-based activated carbon via microwave radiation. J Taiwan Inst Chem E 64, 235–243.
Ge, J., Shen, X., Wu, Z., Wang, P., Wu, X., Li, L., 2019. Effects of K^+, Na^+ and Ca^{2+} coexisting ions on the adsorption of Cr(VI) by activated carbon. Environmental Pollution & Control 41 (1), 6–9.
Giraudet, S., Boulinguiez, B., Le Cloirec, P., 2014. Adsorption and electrothermal desorption of volatile organic compounds and siloxanes onto an activated carbon fiber cloth for biogas purification. Energy Fuel. 28 (6), 3924–3932.
Lashaki, M.J., Fayaz, M., Wang, H.H., Hashisho, Z., Philips, J.H., Anderson, J.E., Nichols, M., 2012. Effect of adsorption and regeneration temperature on irreversible adsorption of organic vapors on beaded activated carbon. Environ. Sci. Technol. 46 (7), 4083–4090.
Li, J., Li, X., Li, M., Lu, S., Yan, J., Xie, W., Liu, C., Qi, Z., 2016. Influence of air pollution control devices on the polycyclic aromatic hydrocarbon distribution in flue gas from an ultralow-emission coal-fired power plant. Energy Fuel. 30 (11), 9572–9579.
Li, J., Qi, Z., Li, M., Wu, D., Zhou, C., Lu, S., Yan, J., Li, X., 2017. Physical and chemical characteristics of condensable particulate matter from an ultralow-emission coal-fired power plant. Energy Fuel. 31 (2), 1778–1785.
Li, X., Zhou, C., Li, J., Lu, S., Yan, J., 2019. Distribution and emission characteristics of filterable and condensable particulate matter before and after a low-low temperature electrostatic precipitator. Environ. Sci. Pollut. Res. 26 (13), 12798–12806.
Li, J., Li, X., Wang, W., Wang, X., Lu, S., Sun, J., Mao, Y., 2021. Investigation on removal effects and condensation characteristics of condensable particulate matter: field test and experimental study. Sci. Total Environ. 783, 146985.
Liu, S., Wu, Y., Xu, Z., Lu, S., Li, X., 2022. Study on characteristics of organic components in condensable particulate matter before and after wet flue gas desulfurization system of coal-fired power plants. Chemosphere 294, 133668.
Meng, G., Li, A., Zhang, Q., 2007. Studies on the oxygen-containing groups of activated carbon and their effects on the adsorption character. Ion Exch. Adsorpt. (1), 88–94.
Miyoshi, T., Boki, K., Tanada, S., 1976. [Studies on the adsorption removal of ammonia gas. 1) Adsorption of ammonia gas on several kinds of activated carbons (author's transl)]. Sangyo igaku. Japanese journal of industrial health 18 (3), 169–176.
Morino, Y., Chatani, S., Tanabe, K., Fujitani, Y., Morikawa, T., Takahashi, K., Sato, K., Sugata, S., 2018. Contributions of condensable particulate matter to atmospheric organic aerosol over Japan. Environ. Sci. Technol. 52 (15), 8456–8466.
Park, S., Kim, B., 2004. Influence of oxygen plasma treatment on hydrogen chloride removal of activated carbon fibers. J. Colloid Interface Sci. 275 (2), 590–595.
Qi, Z., Li, J., Wu, D., Xie, W., Li, X., Liu, C., 2017. Particulate matter emission characteristics and removal efficiencies of a low-low temperature electrostatic precipitator. Energy Fuel. 31 (2), 1741–1746.
Qian, Q., Gong, C., Zhang, Z., Yuan, G., 2015. Removal of VOCs by activated carbon microspheres derived from polymer: a comparative study. Adsorption 21 (4), 333–341.
Qing, X., Huang, R., Huang, J., Feng, G., Yin, W., Yang, Y., Zhang, M., Zhang, S., 2017. Removal of dioxins in flue gas from a MSWI using two kinds of activated carbons with baghouse filtration. Chinese Journal of Environmental Engineering 11 (3), 1677–1682.
Queiroz, L.S., de Souza, L.K.C., Thomaz, K.T.C., Leite Lima, E.T., Rocha Filho, Da, Do, Nascimento, de Oliveira Pires, L.H., Faial, K.D.C.F., Costa, Da, 2020. Activated carbon obtained from amazonian biomass tailings (acai seed): modification, characterization, and use for removal of metal ions from water. J. Environ. Manag. 270, 110868.
Sabeti, Z., Ansarin, K., Seyedrezazadeh, E., Jafarabadi, M.A., Zafari, V., Dastgiri, S., Shakerkhatibi, M., Gholampour, A., Khamnian, Z., Sepehri, M., Dahim, M., Sharbafi, J., Hakimi, D., 2021. Acute responses of airway oxidative stress, inflammation, and hemodynamic markers to ambient $PM_{2.5}$ and their trace metal contents among healthy adolescences: a panel study in highly polluted versus low polluted regions. Environ. Pollut. 288.
Sheng, L., Tang, Y., Yin, W., Lu, Z., Cui, Q., Chen, H., Wang, H., Yao, H., 2010. Study on adsorption properties of modified activated carbon on NH_3. Chem. Ind. For. Prod. 30 (5), 35–39.
Shou, C., Qi, Z., Xie, W., Zou, Z., Liu, C., Li, M., Li, J., Li, X., Li, W., 2016. Experimental study on engineering application of particulate matter removal characteristics of low-low temperature electrostatic precipitator. Proc. Chin. Soc. Electr. Eng. 36 (16), 4326–4332.
Song, J., Lu, S., Wu, Y., Zhou, C., Li, X., Li, J., 2020. Migration and distribution characteristics of organic and inorganic fractions in condensable particulate matter emitted from an ultralow emission coal-fired power plant. Chemosphere 243, 125346.
Sun, Q., Fang, T., Chen, J., Da, C., 2021. Characteristics of chlorine releasing from coal-fired power plant. Atmosphere-Basel 12 (12).
Tang, Q., Zhang, Z., Zhu, W., Cao, Z., 2005. SO_2 and NO selective adsorption properties of coal-based activated carbons. Fuel 84 (4), 461–465.
United Stated, E.P.A., 2016. Method 202-Determination of Condensable Particulate Emissions from Stationary Sources. Website of The U. S. Environmental Protection Agency, The United States of America.
Wang, G., Deng, J., Ma, Z., Hao, J., Jiang, J., 2018. Characteristics of filterable and condensable particulate matter emitted from two waste incineration power plants in China. Sci. Total Environ. 639, 695–704.
Wang, G., Deng, J., Zhang, Y., Li, Y., Ma, Z., Hao, J., Jiang, J., 2020a. Evaluating airborne condensable particulate matter measurement methods in typical stationary sources in China. Environ. Sci. Technol. 54 (3), 1363–1371.
Wang, K., Yang, L., Li, J., Sheng, Z., He, Q., Wu, K., 2020b. Characteristics of condensable particulate matter before and after wet flue gas desulfurization and wet electrostatic precipitator from ultra-low emission coal-fired power plants in China. Fuel 278, 118206.
Wang, A., Sun, K., Wu, L., Wu, P., Zeng, W., Tian, Z., Huang, Q., 2020c. Co-carbonization of biomass and oily sludge to prepare sulfamethoxazole super-adsorbent materials. Sci. Total Environ. 698, 134238.
Wang, B., Tang, Z., Cai, N., Niu, H., 2021. The characteristics and sources apportionment of water-soluble ions of $PM_{2.5}$ in suburb Tangshan, China. Urban Clim. 35, 100742.
Wu, D., Lin, S., Yang, H., Rong-guang, Du, Xia, J., Qi, B., Liu, G., Li, F., Yang, M., Gai, X., 2017. Pollution characteristics and light extinction contribution of water-soluble ions of $PM_{2.5}$ in hangzhou. Huanjing Kexue 38 (7), 2656–2666.
Wu, Y., Xu, Z., Liu, S., Tang, M., Lu, S., 2021a. Migration and emission characteristics of N-alkanes and phthalates in condensable particulate matter from coal-fired sources. J. Clean. Prod., 127203
Wu, Y., Xu, Z., Liu, S., Tang, M., Lu, S., 2021b. Emission characteristics of $PM_{2.5}$ and components of condensable particulate matter from coal-fired industrial plants. Sci. Total Environ. 796, 148782.

Wu, Y., Xu, Z., Liu, S., Tang, M., Lu, S., 2021c. Emission of organic components and distribution characteristics of PAHs in condensable particulate matter from coal-fired power and industrial plants. J. Energy Inst. 97, 109–116.
Xu, Z., Wu, Y., Liu, S., Tang, M., Lu, S., 2022. Distribution and emission characteristics of filterable and condensable particulate matter in the flue gas emitted from an ultra-low emission coal-fired power plant. J. Environ. Chem. Eng. 10 (3), 107667.
Yahya, M.A., Al-Qodah, Z., Ngah, C.W.Z., 2015. Agricultural bio-waste materials as potential sustainable precursors used for activated carbon production: a review. Renew. Sustain. Energy Rev. 46, 218–235.
Yang, H., Arafath, S.M., Lee, K., Hsieh, Y., Han, Y., 2018. Chemical characteristics of filterable and condensable PM2.5 emissions from industrial boilers with five different fuels. Fuel 232, 415–422.
Yang, H., Gupta, S.K., Dhital, N.B., Lee, K., Hsieh, Y., Huang, S., 2019. Establishment of indicatory metals for filterable and condensable $PM_{2.5}$ emitted from important stationary emission sources. Energy Fuel. 33 (11), 10878–10887.
Zhang, J., 2008. Experimental Study on Simultaneous Desulfurization and Denitrification over Activated Carbon Fibers. Xi'an University of Architecture and Technology, p. 61.
Zhang, X., Gao, B., Creamer, A.E., Cao, C., Li, Y., 2017. Adsorption of VOCs onto engineered carbon materials: a review. J. Hazard Mater. 338, 102–123.
Zhang, X., Li, Y., Zhang, Z., Nie, M., Wang, L., Zhang, H., 2021. Adsorption of condensable particulate matter from coal-fired flue gas by activated carbon. Sci. Total Environ. 778, 146245.
Zheng, C., Hong, Y., Liu, S., Yang, Z., Chang, Q., Zhang, Y., Gao, X., 2018. Removal and emission characteristics of condensable particulate matter in an ultralow emission power plant. Energy Fuel. 32 (10), 10586–10594.
Zhou, H., Zhong, Z., Jin, B., Huang, Y., Xiao, R., 2005. Experimental study on the removal of PAHs using in-duct activated carbon injection. Chemosphere 59 (6), 861–869.
Zhu, D., 2015. Studies on Absorption of SO_2 and NO_X by Activated Carbon. Huazhong University of Science and Technology, p. 64.